Spectrochimica Acta Part B 105 (2015) 116–120

Contents lists available at ScienceDirect

Spectrochimica Acta Part B

journal homepage: www.elsevier.com/locate/sab

Validation of the determination of the B isotopic composition in Roman glasses with laser ablation multi-collector inductively coupled plasma-mass spectrometry ☆

Veerle Devulder [a,b], Axel Gerdes [c], Frank Vanhaecke [a,*], Patrick Degryse [b]

[a] Department of Analytical Chemistry, Ghent University, Krijgslaan 281-S12, 9000 Ghent, Belgium
[b] Department of Earth and Environmental Sciences, Katholieke Universiteit Leuven, Celestijnenlaan 200 E-box 2408, 3001 Leuven, Belgium
[c] Institute of Geoscience, Goethe Universität, Altenhoeferallee 1, 60438 Frankfurt am Main, Germany

ARTICLE INFO

Article history:
Received 17 April 2014
Accepted 21 August 2014
Available online 16 October 2014

Keywords:
Isotopic analysis
Boron
Laser ablation
Multi-collector ICP-mass spectrometry
Provenance determination
Ancient glass
Isotope fractionation

ABSTRACT

The applicability of laser ablation multi-collector inductively coupled plasma-mass spectrometry (LA-MC-ICP-MS) for the determination of the B isotopic composition in Roman glasses was investigated. The $\delta^{11}B$ values thus obtained provide information on the natron flux used during the glass-making process. The glass samples used for this purpose were previously characterized using pneumatic nebulization (PN) MC-ICP-MS. Unfortunately, this method is time-consuming and labor-intensive and consumes some 100 mg of sample, which is a rather high amount for ancient materials. Therefore, the use of the less invasive and faster LA-MC-ICP-MS approach was explored. In this work, the results for 29 Roman glasses and 4 home-made glasses obtained using both techniques were compared to assess the suitability of LA-MC-ICP-MS in this context. The results are in excellent agreement within experimental uncertainty. No difference in overall mass discrimination was observed between the Roman glasses, NIST SRM 610 reference glass and B6 obsidian. The expanded uncertainty of the LA-MC-ICP-MS approach was estimated to be <2‰, which is similar to that obtained upon sample digestion and PN-MC-ICP-MS measurement.

1. Introduction

Isotopic analysis of B is traditionally carried out using thermal ionization mass spectrometry (TIMS) [1–3], or more recently, multi-collector ICP-mass spectrometry (MC-ICP-MS) [4–7]. Prior to such analysis, the sample needs to be digested and B separated from the concomitant matrix elements. This wet chemistry procedure, however, is very laborious and time-consuming; the whole procedure takes 2 weeks on average. Moreover, no spatially resolved information is obtained, which could be of interest, e.g., in the context of analysis of foraminifera or corals for paleo-pH reconstruction [8,9]. These disadvantages can be circumvented by in situ measurements. Direct analysis of solid samples has the advantage of reducing the work load in terms of sample preparation and thus, offers an enhanced sample throughput. Also spatially resolved analysis is enabled in this way. The two techniques currently used for in situ measurement of the B isotope ratio are secondary ion mass spectrometry (SIMS) and laser ablation (LA) MC-ICP-MS. For SIMS, close matrix-matching is an absolute prerequisite for obtaining accurate results [10]. In the case of the more recently introduced LA-MC-ICP-MS approach for B isotopic analysis, matrix matching seems to be less demanding [8,11,12], although recently a close matrix matching was reported to be necessary for B isotope ratio determination in tourmalines using a 213 nm Nd:YAG laser [13]. Also the precision obtained using LA-MC-ICP-MS (<1‰ 2SD) is better than that obtained with SIMS (3‰ 2SD) [8,14]. Of course, the precision depends on the heterogeneity of the matrix. To the best of the authors' knowledge, only 5 papers have reported on LA-MC-ICP-MS isotopic analysis of B in geological materials thus far [8,11,13,15,16]. Additionally, Kurta et al. [12] have reported the use of femtosecond-LA-MC-ICP-MS for the screening of B isotope ratios in steel.

Also in archeometry, especially for ancient glass, B isotopic analysis using LA-MC-ICP-MS would be of great interest. Recently, it has been demonstrated that the B isotope ratio can provide information on the source of flux raw material used in the production of Roman natron glass [17]. Different flux materials were used in glass production: natron or plant ash. Natron glasses were widespread in the Mediterranean and the Levant between the first millennium BC and the ninth century AD, while plant ash glasses were produced before the first millennium BC and after the ninth century AD [18,19]. These different fluxes are expected to give different B isotope ratios, while at least for natron, the B isotopic composition also provides information on the geographical

☆ This article is dedicated to Jim Holcombe, in recognition of his academic, mentoring and scientific achievements, and his service to the spectroscopic community.

* Corresponding author.
E-mail address: Frank.Vanhaecke@UGent.be (F. Vanhaecke).

http://dx.doi.org/10.1016/j.sab.2014.08.038

provenance [20]. However, the wet chemistry procedure preceding B isotopic analysis via MC-ICP-MS includes target element isolation via microsublimation [21] or chromatographic isolation and is therefore very tedious and time-consuming and requires a relatively large amount of precious sample (ca. 100 mg). As the use of LA-MC-ICP-MS would reduce the work load and reduce the amount of sample required, it is very attractive. In this paper, the use of LA-MC-ICP-MS for the analysis of 29 Roman (both natron and plant ash) glasses and 4 home-made glasses [22] is described and the results thus obtained compared to those obtained using PN-MC-ICP-MS. The influence of the matrix is addressed and the expanded uncertainty estimated.

2. Experimental

2.1. Reagents and instrumentation

All reagents and instrumentation used for PN-MC-ICP-MS analysis are described in Devulder et al. [17]. For LA-MC-ICP-MS analysis, NIST SRM 610 glass (National Institute for Standards and Technology, MD, USA) was used as standard and B6 obsidian as a quality control sample. For practical purposes, all glass samples (micrometer size) were mounted in epoxy resin (<0.1 ppm B) and polished. The RESOlution M-50-LR (Resonetics) LA-unit used is based on an ArF* excimer laser (CompexPro 102, Coherent), providing a high-energy 193 nm laser beam, and is equipped with a dual volume M50 LA cell (Laurin Technic, Australia), as described in Mueller et al. [23]. The sample was ablated under He atmosphere and the sample stream coming from the ablation cell was admixed with Ar and N_2 prior to its introduction into the ICP to stabilize the signal [24]., prior to its introduction into the ICP. A *squid* device [23] (Laurin Technic, Australia) was placed between the ablation cell and the ICP to smooth the signals. The MC-ICP-mass spectrometer used is a Neptune (Thermo Scientific, Germany), equipped with 9 Faraday cups connected to 10^{11} Ω amplifiers. Table 1 summarizes the instrument settings of both the laser ablation unit and the MC-ICP-MS unit, as well as the data acquisition parameters used. Table 2 describes the cup configuration used.

Table 1
Instrument settings and data acquisition parameters for B isotope ratio measurement via LA-MC-ICP-MS (RESOlution M-50 and Thermo Scientific Neptune), optimized daily for highest stability and signal intensity.

Instrument settings: Laser	
Wavelength (nm)	193
Cell volume (cm^3)	Box volume: 380 Effective volume: 1–2
Spot size (μm)	Depending on concentration of the sample (ranging between 40 and 240)
Frequency (Hz)	8
Energy density (J cm^{-2})	2.5
Carrier (He) gas flow rate through cell ($L.min^{-1}$)	0.6
N_2 gas flow rate ($mL.min^{-1}$)	3.5
Instrument settings: Neptune	
RF power (W)	1320
Cool gas flow rate ($L \cdot min^{-1}$)	15.5
Auxiliary gas flow rate ($L \cdot min^{-1}$)	0.85
Sampler cone	Ni
Skimmer	Ni, X-type
X-position (mm)	−2.21
Y-position (mm)	−1.12
Z-position (mm)	−4.79
Resolution	Low
Data acquisition parameters: Neptune	
Integration time (s)	0.524
Blocks	6–12
Cycles/block	3800

Table 2
Cup configuration used for B isotope ratio measurements using LA-MC-ICP-MS.

L4	L3	L2	L1	C	H1	H2	H3	H4
		^{10}B		10.537		^{11}B		

The measurement sequence consisted of a series of measurements of the standard and quality control sample (NIST SRM 610, B6), followed by a block of samples. At the beginning of the sequence, NIST SRM 610 glass was measured using different spot sizes. This was required to cope with the large B concentration range within the sample collection. For each sample, a proper spot size was selected taking into account its B concentration. Spot sizes were chosen such that the intensity of the ^{11}B signals was around 0.3 V. 3 to 5 samples were measured in-between successive measurements of NIST SRM 610 glass. Per sample, 6 to 12 spots were analyzed. The laser repetition frequency was set to 8 Hz. At each location, first, a gas blank was measured for 12 s. Subsequently, the sample surface was pre-ablated (4 shots) and the gas blank was measured during another 30 s. Finally, the sample was measured for 27 s. The data acquisition was continuous (i.e. even during the measurement of the gas blanks and pre-ablation) and all data treatments were done offline.

2.2. Samples

33 glass samples were measured via LA-MC-ICP-MS. These samples are Greco–Roman natron glasses, plant ash glasses and home-made glasses [22]. From PN-MC-ICP-MS measurements, it was known that the $\delta^{11}B$ values ranged from −10 to +40‰ and the B concentrations ranged from 10 to 1000 $\mu g \cdot g^{-1}$. The sample descriptions and their B isotopic composition as obtained via PN-MC-ICP-MS are provided in Table 3.

2.3. Data treatment and corrections

All data treatments were done offline. The average gas blank level was subtracted from the ^{11}B and ^{10}B intensities for the sample. Then, the $^{11}B/^{10}B$ ratios were calculated and outliers were removed based on a 2 s-test. Correction for mass discrimination was accomplished via external calibration using a sample-standard (NIST SRM 610) bracketing approach. A linear variation of the extent of mass discrimination was assumed in-between successive measurements of the NIST SRM 610 standard. The $^{11}B/^{10}B$ value used for NIST SRM 610 is 4.052 ± 0.0008 (2SD) and is based on 11 measurements of NIST SRM 610 relative to NIST SRM 612 on the day of analysis. The $\delta^{11}B$ value used for NIST SRM 612 is −1.07 ± 1.7‰ (2SD) (N = 7), as in Kasemann et al. [25]. It was also necessary to correct for the different spot sizes used during ablation. This correction was based on the linear relation observed between the mass discrimination-corrected $^{11}B/^{10}B$ isotope ratio and spot size for NIST SRM 610 glass (Fig. 1). The ratio thus obtained is then expressed as a $\delta^{11}B$ value vs. NIST SRM 951, using 4.0545 as the $^{11}B/^{10}B$ ratio for this isotopic reference material, according to Kasemann et al. [25]. The result of the sample is then the average of the ratios of all spots analyzed. It should be noted that the variation between the $\delta^{11}B$ results for spots of 1 sample is relatively small (0.5‰, 2SD) (Table 3).

3. Results and discussion

The $\delta^{11}B$ results obtained via PN-MC-ICP-MS and LA-MC-ICP-MS are presented in Fig. 2. It can be seen that the results are in very good agreement with each other. However, depending on the reference values used for NIST SRM 610 and NIST SRM 951, different results are obtained, as can be seen in Fig. 3. In this figure, "LA" refers to the results obtained using the calculation described above (these results are included in Fig. 2), "Le Roux" and "Kasemann" refer to the LA-MC-ICP-MS results obtained using the values for NIST SRM 610 and NIST SRM 951 as reported in le Roux et al. (4.049 and 4.05003) [16] and Kasemann et al.

Table 3
Information on the samples analyzed, their origin, color, B concentration and $\delta^{11}B$ (‰) as determined using PN-MC-ICP-MS [20] as well as the number of spots measured for laser ablation (LA) and the obtained average values with their corresponding 2SD.

Sample	Color	Date[a]	Sample location	[B] ($\mu g \cdot g^{-1}$)	$\delta^{11}B$ (‰)	Number of spots for LA	$\delta^{11}B$ (‰) ± 2SD LA
SA-2007-VL-358	Colorless	Second half 2nd century	Sagalassos	195	30.1	9	29.9 ± 0.4
SA-2007-VL-1161	Yellow	1st–7th centuries AD	Sagalassos	253	32.6	9	33.8 ± 0.2
SA-2007-VL-744	Colorless	1st–7th centuries AD	Sagalassos	139	29.7	6	30.1 ± 0.2
SA-2007-VL-678	Colorless	1st–7th centuries AD	Sagalassos	161	30.2	9	29.7 ± 0.4
SA-2007-VL-219	Colorless	1st half 4th century AD	Sagalassos	162	28.7	6	28.7 ± 0.5
SA-2007-VL-135	Colorless	2nd half 4th century, 1st half 5th century AD	Sagalassos	150	28.7	7	28.4 ± 1.4
SA-2007-VL-539	Yellow/green	1st–7th centuries AD	Sagalassos	238	29.4	7	28.3 ± 0.5
SA-2007-VL-115	Colorless	1st–7th centuries AD	Sagalassos	148	29.7	5	29.6 ± 0.4
SA-2007-VL-211	Colorless	1st–7th centuries AD	Sagalassos	151	27.3	8	26.8 ± 0.6
SA-2007-VL-304	Pale yellow	1st–7th centuries AD	Sagalassos	158	27.1	8	27.0 ± 0.3
SA-2006-VL-7	Colorless	End 5th century AD/6th century AD	Sagalassos	210	28.8	7	29.0 ± 0.4
SA-2007-VL-26	Dark blue	1st–7th centuries AD	Sagalassos	163	30.1	7	30.2 ± 1.3
SA-2005-VL-31	Brown	1st–7th centuries AD	Sagalassos	171	31.0	7	31.1 ± 1.2
SA-2007-VL-1167	Pale green	1st–7th centuries AD	Sagalassos	177	27.1	7	27.8 ± 0.5
SA-2007-VL-1085	Colorless	1st–7th centuries AD	Sagalassos	167	27.7	7	28.5 ± 0.8
SA-2007-VL-1095	Yellow	1st–7th centuries AD	Sagalassos	291	32.2	7	32.6 ± 0.4
8933	Pale blue/green	4th–5th centuries AD	Oudenburg	160	28.7	12	29.7 ± 0.3
8926 C	Pale blue/green	3rd century AD	Oudenburg	136	29.7	10	30.0 ± 0.5
71310	Pale blue	3rd century AD	Oudenburg	154	28.2	9	28.6 ± 0.4
23993	Pale blue/green	4th–5th centuries AD	Oudenburg	160	28.7	9	28.7 ± 0.6
2960	Pale blue	4th–5th centuries AD	Oudenburg	194	27.4	11	27.8 ± 0.6
SA-2006-VL-05	Yellow/green	1st–7th centuries AD	Sagalassos	265	27.4	9	26.8 ± 0.2
SA-2007-VL-137	HIMT	1st–7th centuries AD	Sagalassos	199	27.7	8	28.0 ± 0.4
SA-2007-VL-138	HIMT	1st–7th centuries AD	Sagalassos	188	26.9	8	27.8 ± 0.3
RBS 067	Opaque red/brown	11th–12th centuries	Sagalassos	2658	−6.5	7	−7.5 ± 0.3
RBS 070	Pale purple/pink	12th–13th centuries	Sagalassos	84	35.6	6	36.9 ± 0.2
RBS 072	Dark blue	1st–6th and 12th–13th centuries	Sagalassos	2868	−7.1	9	−8.0 ± 0.4
RBS 073	Blue	5th century/middle Byzantine	Sagalassos	2771	−7.7	8	−8.7 ± 0.3
RBS 075	Green	Middle Byzantine and 1st–5th century material	Sagalassos	3040	−6.4	8	−6.9 ± 0.6
FR16	Blue	Manufactured by Brems et al. [22]		14	−7.8	8	−7.1 ± 1.2
IT85	Green			15	−8.0	9	−8.0 ± 0.4
IT34	Pale green			13	−5.6	9	−3.8 ± 0.6
IT87	Pale green			5	+0.4	6	2.4 ± 0.3

[a] References for these dates can be found in Devulder et al. [20].

(4.051 and 4.0545) [25], respectively. Whatever reference values are used, the LA-MC-ICP-MS results are not significantly different from the corresponding PN-MC-ICP-MS data. It has to be noted that two of the previously published papers [11,15] use 4.049 as the reference value for NIST SRM 610, as determined by le Roux et al. [16]. However, the value for NIST SRM 951 used in all three papers is 4.05003, which is not determined by le Roux et al., but by Ishikawa and Tera [26]. The value of Kasemann et al. [25] for NIST SRM 610 is −0.78‰ (P-TIMS) and that for NIST SRM 612 −1.07‰. In contrast to le Roux et al., Kasemann et al. also measured the value for NIST SRM 951, reported as 4.0545. Therefore, the value reported by Kasemann et al. was used for both NIST SRM 612 and NIST SRM 951 in this work, as in the authors' opinion, these values are more reliable. NIST SRM 610 was measured repeatedly relative to NIST SRM 612 and the measured value was then used for calculating the $\delta^{11}B$ values of the samples using 4.0545 as a reference $^{11}B/^{10}B$ value for NIST SRM 951. The average measured value for NIST SRM 610 is −0.56 ± 0.32‰, which is very close to the average (−0.52‰) of the values determined by le Roux et al. (−0.25 ± 0.28‰, 2SD, N = 2), by Kasemann et al. (−0.78 ± 1.4‰, 2SD, N = 8, P-TIMS) and by Fietzke et al. [8] (−0.55 ± 1‰, 2SD, N = 16). Overall, the relative difference between the results obtained using the lowest

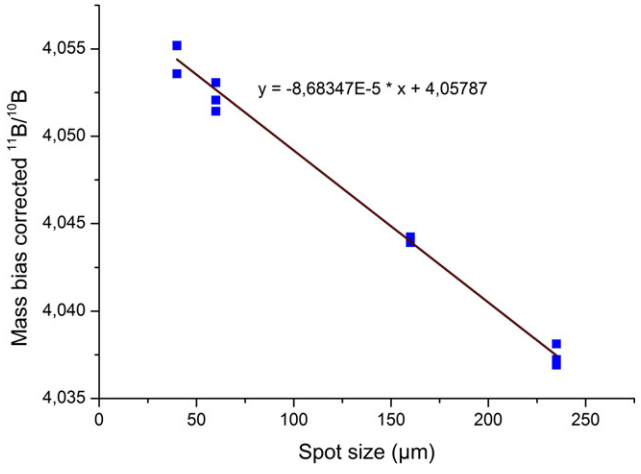

Fig. 1. Dependence of $^{11}B/^{10}B$ ratio on spot size (μm) for NIST SRM 610 glass.

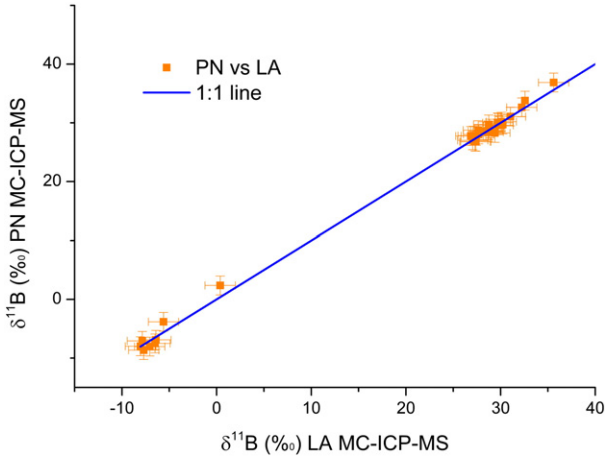

Fig. 2. Comparison of the $\delta^{11}B$ (‰) results obtained using PN-MC-ICP-MS and LA-MC-ICP-MS. The uncertainty on the PN-MC-ICP-MS results is 1.6‰ (k = 2), as determined in Devulder et al. [17].

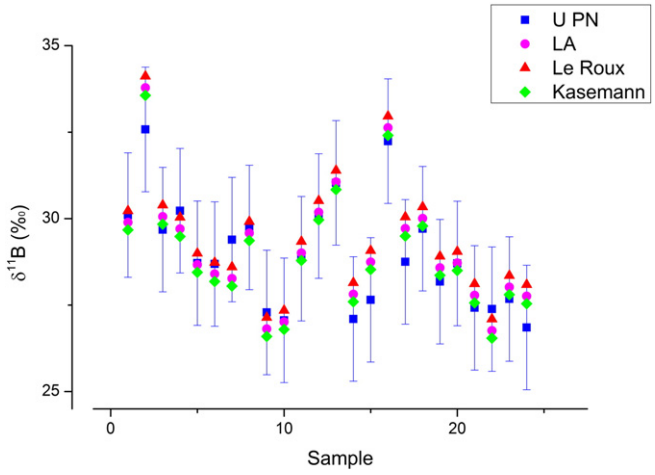

Fig. 3. Influence of the use of different reference values for NIST SRM 610 to calculate the results obtained by LA-MC-ICP-MS. "U PN" is the expanded uncertainty accompanying the PN-MC-ICP-MS results, "LA" refers to the LA-MC-ICP-MS results obtained relying on the experimentally determined value of 4.052 for NIST SRM 610. "Le Roux" and "Kasemann" refer to the LA-MC-ICP-MS results obtained using the average values of 4.049 and 4.051 for NIST SRM 610, as reported by le Roux et al. [16] and Kasemann et al. (P-TIMS) [25], respectively.

(−0.78‰) [25] and the highest δ-value (−0.25‰) [16] for NIST SRM 610 is only 0.53‰. When comparing this value to the expanded uncertainty obtained for PN-MC-ICP-MS (1.6‰, k = 2), it can be seen that this difference is negligible.

No matrix effect – defined as a difference in the overall extent of mass discrimination – is observed for archeological glasses or B6 obsidian when compared to NIST SRM 610 glass. The $\delta^{11}B$ value obtained for B6 obsidian is −2.59 ± 0.50‰ (N = 18), which is within experimental uncertainty equal to our PN-MC-ICP-MS value [17] (−2.89 ± 1.6‰, N = 8), the result obtained by Hou et al. [11] (−3.29 ± 1.12‰) and the average of the results from an intercomparison exercise in 2003 [27] (−3.3 ± 1.8‰). Moreover, all of the $\delta^{11}B$ results for the archeological glasses are in excellent agreement with the corresponding PN-MC-ICP-MS $\delta^{11}B$ values.

The comparison of the expanded uncertainty of both methods is challenging, especially since assessing the accuracy of the LA-MC-ICP-MS results is difficult. This is due to the lack of a certified reference material. NIST SRM 610 glass resembles the matrix of the archeological glasses, but there are only indicative $\delta^{11}B$ values available. These values differ from one lab to another and also depend on the $\delta^{11}B$ value used for NIST SRM 951. le Roux et al. [16] mention an average $\delta^{11}B$ value of −0.25‰ for NIST SRM 610, based on a $^{11}B/^{10}B$ ratio for NIST SRM 951 of 4.05003. Kasemann et al. [25], on the other hand, reported a $\delta^{11}B$ value for NIST SRM 610 of −0.78‰ based on a $^{11}B/^{10}B$ ratio of 4.0545 for NIST SRM 951. Fortunately, all results are identical within analytical uncertainty, thus enabling the uncertainty on the bias of our LA-MC-ICP-MS to be calculated. The bias on the true value is assumed to be at least 0.53‰ as this is the difference between the results of different labs. Next to the bias, the top down approach for determining the expanded uncertainty also uses the intermediate precision. According to the VIM [28], the intermediate precision is *the measurement precision under a set of conditions that includes the same measurement procedure, same location and replicate measurement on the same or similar objects over an extended period of time, but may include other conditions involving changes*. 3 samples, each measured on at least 4 spots, were measured on 2 separate days with one month in-between. It has to be noted that the results of the 3 samples measured on both days result in an excellent intermediate precision (0.3‰). Moreover, the standard deviation on all NIST SRM 610 glass measurement results of one day (NIST SRM 610 was measured 38 times during a time span of 11 h) was only 0.23‰. It should be noted that the intermediate precision using LA-MC-ICP-MS (0.3‰) is better than the precision of the PN-MC-ICP-MS procedure (0.6‰). Due to the lack of a certified value for determining the bias, deploying a similar or slightly lower expanded uncertainty for LA-MC-ICP-MS as for pneumatic nebulization MC-ICP-MS seems justified. Overall, it can be concluded that the LA-MC-ICP-MS results are the same as the pneumatic nebulization results within analytical uncertainty and no systematic matrix-induced offset is observed.

4. Conclusion

Reliable B isotopic analysis of ancient glass samples, showing a broad B concentration range and a broad $\delta^{11}B$ range, was accomplished using LA-MC-ICP-MS. The LA-MC-ICP-MS results were in excellent agreement with those obtained via PN-MC-ICP-MS after labor-intensive and time-consuming sample pretreatment (digestion and chromatographic B isolation). No matrix-induced changes in the extent of mass discrimination have been observed between NIST SRM 610 glass, B6 obsidian and archeological glasses. The $^{11}B/^{10}B$ result depends on the spot size and thus, normalization should form an integral part of the data processing. Due to the lack of certified reference materials for $\delta^{11}B$, the expanded uncertainty of the LA-MC-ICP-MS approach could not be calculated exactly, however, it is estimated to be similar to that typical for PN-MC-ICP-MS and amounts to 1.6‰ with a coverage factor k of 2. The method is ready to be used for analyzing larger collections of natron glass. The success of provenancing depends on the availability and spread of the reference values for possible natron sources.

Acknowledgments

The ERC Starting Grant ARCHGLASS (grant agreement no. 240750) is acknowledged for financial support. The Flemish Research Foundation (FWO-Vlaanderen) is acknowledged for financial support through Research Project G002111N. Sonia Tonarini is thanked for providing the B6 obsidian piece.

References

[1] S. Barth, Boron isotopic analysis of natural fresh and saline waters by negative thermal ionization mass spectrometry, Chem. Geol. 143 (1997) 255–261.
[2] A.J. Spivack, J.M. Edmond, Determination of boron isotope ratios by thermal ionization mass-spectrometry of the dicesium metaborate cation, Anal. Chem. 58 (1986) 31–35.
[3] T. Nakano, E. Nakamura, Static multicollection of $Cs_2BO_2^+$ ions for precise boron isotope analysis with positive thermal ionization mass spectrometry, Int. J. Mass Spectrom. 176 (1998) 13–21.
[4] C. Lecuyer, P. Grandjean, B. Reynard, F. Albarede, P. Telouk, B-11/B-10 analysis of geological materials by ICP-MS Plasma 54: application to the boron fractionation between brachiopod calcite and seawater, Chem. Geol. 186 (2002) 45–55.
[5] J.K. Aggarwal, D. Sheppard, K. Mezger, E. Pernicka, Precise and accurate determination of boron isotope ratios by multiple collector ICP-MS: origin of boron in the Ngawha geothermal system, New Zealand, Chem. Geol. 199 (2003) 331–342.
[6] P. Louvat, J. Bouchez, G. Paris, MC-ICP-MS isotope measurements with direct injection nebulisation (d-DIHEN): optimisation and application to boron in seawater and carbonate samples, Geostand. Geoanal. Res. 35 (2011) 75–88.
[7] C. Guerrot, R. Millot, M. Robert, P. Negrel, Accurate and high-precision determination of boron isotopic ratios at low concentration by MC-ICP-MS (Neptune), Geostand. Geoanal. Res. 35 (2011) 275–284.
[8] J. Fietzke, A. Heinemann, I. Taubner, F. Bohm, J. Erez, A. Eisenhauer, Boron isotope ratio determination in carbonates via LA-MC-ICP-MS using soda-lime glass standards as reference material, J. Anal. At. Spectrom. 25 (2010) 1953–1957.
[9] C. Rollion-Bard, J. Erez, Intra-shell boron isotope ratios in the symbiont-bearing benthic foraminiferan *Amphistegina lobifera*: implications for delta B-11 vital effects and paleo-pH reconstructions, Geochim. Cosmochim. Acta 74 (2010) 1530–1536.
[10] M. Rosner, M. Wiedenbeck, T. Ludwig, Composition-induced variations in SIMS instrumental mass fractionation during boron isotope ratio measurements of silicate glasses, Geostand. Geoanal. Res. 32 (2008) 27–38.
[11] K. Hou, Y. Li, Y. Xiao, F. Liu, Y. Tian, In situ boron isotope measurements of natural geological materials by LA-MC-ICP-MS, Chin. Sci. Bull. 55 (2010) 3305–3311.
[12] C. Kurta, L. Dorta, F. Mittermayr, K. Prattes, B. Hattendorf, D. Günther, W. Goessler, Rapid screening of boron isotope ratios in nuclear shielding materials by LA-ICPMS—a comparison of two different instrumental setups, J. Anal. At. Spectrom. 29 (2014) 185–192.
[13] J. Mikova, J. Kosler, M. Wiedenbeck, Matrix effects during laser ablation MC ICP-MS analysis of boron isotopes in tourmaline, J. Anal. At. Spectrom. 29 (2014) 903–914.

[14] M. Chaussidon, F. Albarede, Secular boron isotope variations in the continental-crust — an ion microprobe study, Earth Planet. Sci. Lett. 108 (1992) 229–241.
[15] M. Tiepolo, C. Bouman, R. Vannucci, J. Schwieters, Laser ablation multicollector ICPMS determination of delta B-11 in geological samples, Appl. Geochem. 21 (2006) 788–801.
[16] P.J. le Roux, S.B. Shirey, L. Benton, E.H. Hauri, T.D. Mock, In situ, multiple-multiplier, laser ablation ICP-MS measurement of boron isotopic composition (delta B-11) at the nanogram level, Chem. Geol. 203 (2004) 123–138.
[17] V. Devulder, P. Degryse, F. Vanhaecke, Development of a novel method for unraveling the origin of natron flux used in Roman glass production based on B isotopic analysis via multi-collector ICP-mass spectrometry, Anal. Chem. 85 (2013) 12077–12084.
[18] I.C. Freestone, M. Ponting, M.J. Hughes, The origins of Byzantine glass from Maroni Petrera, Cyprus, Archaeometry 44 (2002) 257–272.
[19] A. Shortland, L. Schachner, I. Freestone, M. Tite, Natron as a flux in the early vitreous materials industry: sources, beginnings and reasons for decline, J. Archaeol. Sci. 33 (2006) 521–530.
[20] V. Devulder, F. Vanhaecke, A. Shortland, D.J. Mattingly, C.M. Jackson, P. Degryse, Boron isotopic composition as a provenance indicator for the flux raw material in Roman natron glass, J. Archaeol. Sci. 46 (2014) 107–113.
[21] B.S. Wang, C.F. You, K.F. Huang, S.F. Wu, S.K. Aggarwal, C.H. Chung, P.Y. Lin, Direct separation of boron from Na- and Ca-rich matrices by sublimation for stable isotope measurement by MC-ICP-MS, Talanta 82 (2010) 1378–1384.
[22] D. Brems, P. Degryse, M. Ganio, S. Boyen, The production of Roman glass with western Mediterranean sand raw materials: preliminary results, Glass Technol. Eur. J. Glass Sci. Technol. Part A 53 (2012) 129–138.
[23] W. Mueller, M. Shelley, P. Miller, S. Broude, Initial performance metrics of a new custom-designed ArF excimer LA-ICPMS system coupled to a two-volume laser-ablation cell, J. Anal. At. Spectrom. 24 (2009) 209–214.
[24] D. Beauchemin, J.M. Craig, Investigations on mixed-gas plasmas produced by adding nitrogen to the plasma gas in ICP-MS, Spectrochim. Acta Part B 46 (1991) 603–614.
[25] S. Kasemann, A. Meixner, A. Rocholl, T. Vennemann, M. Rosner, A.K. Schmitt, M. Wiedenbeck, Boron and oxygen isotope composition of certified reference materials NIST SRM 610/612 and reference materials JB-2 and JR-2, Geostand. Newsl. J. Geostand. Geoanal. 25 (2001) 405–416.
[26] T. Ishikawa, F. Tera, Source, composition and distribution of the fluid in the Kurile mantle wedge: constraints from across-arc variations of B/Nb and B isotopes, Earth Planet. Sci. Lett. 152 (1997) 123–138.
[27] R. Gonfiantini, S. Tonarini, M. Groning, A. Adorni-Braccesi, A.S. Al-Ammar, M. Astner, S. Bachler, R.M. Barnes, R.L. Bassett, A. Cocherie, A. Deyhle, A. Dini, G. Ferrara, J. Gaillardet, J. Grimm, C. Guerrot, U. Krahenbuhl, G. Layne, D. Lemarchand, A. Meixner, D.J. Northington, M. Pennisi, E. Reitznerova, I. Rodushkin, N. Sugiura, R. Surberg, S. Tonn, M. Wieclenbeck, S. Wunderli, Y.K. Xiao, T. Zack, Intercomparison of boron isotope and concentration measurements. Part II: evaluation of results, Geostand. Newsl. J. Geostand. Geoanal. 27 (2003) 41–57.
[28] JCGM, International vocabulary of metrology — basic and general concepts and associated terms (VIM), BIPM, 2008.